RAS M-236

NEC-JH_72

Paper 96. The influence of oxygen and hydrazine on the erosion-corrosion behaviour and electrochemical potentials of carbon steel under boiler feedwater conditions

I. S. WOOLSEY, BSc, PhD, G. J. BIGNOLD, BSc, PhD, C. H. DE WHALLEY, BSc, MIChemE, and K. GARBETT, BSc, PhD, CEGB, Central Electricity Research Laboratories, Leatherhead

In the temperature range 100 to 250°C, carbon steel is highly susceptible to erosion-corrosion damage in deoxygenated boiler feedwater when mass transfer coefficients are sufficiently high. The erosion-corrosion process can be completely inhibited by addition of low levels of oxygen to the feedwater, but experiments have shown that the process continues essentially unaffected below a critical oxygen threshold. The oxygen level required to inhibit the process depends on the local oxygen mass transfer coefficient to the eroding surface, and the existing metal loss rate. An upper limit for the threshold concentration can be derived from the rate of oxygen mass transfer to the surface required to match the ongoing erosion-corrosion rate. Under these circumstances, the cathodic current normally supplied by the hydrogen evolution reaction can be substituted by an equivalent one due to oxygen reduction. When the critical rate of oxygen mass transfer to the surface required to inhibit erosion corrosion is achieved, the surface electrochemical potential shifts several hundred millivolts positive of that previously maintained. Oxygen has been shown to inhibit erosion-corrosion and control the electrochemical potential of carbon steel even in the presence of large excesses of reducing agents such as N_2H_4 and H_2, at temperatures up to 250°C. However, removal of the oxygen by reaction with hydrazine allows the erosion-corrosion process to re-initiate rapidly. Hydrazine alone does not significantly influence the potential of actively eroding surfaces, but does appear to reduce the erosion-corrosion rate as a result of the increased high temperature pH.

INTRODUCTION

1. In the temperature range 100 to 250°C, carbon steel is highly susceptible to erosion-corrosion damage in deoxygenated boiler feedwater if fluid velocities and hence mass transfer coefficients are high enough (ref. 1). However, oxygen in the feedwater has an inhibiting effect on the erosion-corrosion process (ref. 2 to 5), to the extent that when oxygen levels are high enough, the attack is completely suppressed. However, the exact amount of oxygen required, in general, to inhibit the process under a given set of conditions has not been established.

2. Various feedwater chemistries have been developed in recent years which utilise oxygen dosing at some level which would be expected to be successful in suppressing erosion-corrosion damage under single phase flow conditions. The NOLC, Neutral Oxygen Low Conductivity (ref. 6) and Combined Oxygen-Ammonia (ref. 7) water chemistry regimes employ relatively high levels of oxygen in the feedwater, without or with ammonia dosing respectively. Specifications for the NOLC regime require >50 μg kg^{-1} oxygen (ref. 6), whilst the combined regime has been optimised with oxygen levels in the range 150 to 300 μg kg^{-1} and ammonia dosing to give a pH_{25}°C between 8.0 and 8.5 (ref. 7). However, a variation of the combined regime adopted for CEGB gas cooled reactor once-through boilers employs much lower levels of oxygen dosing, 15 μg kg^{-1}, with a pH_{25}°C from ammonia >9.3. It removed in the higher temperature sections of the boiler. This is to eliminate its possible influence on corrosion in the 9Cr1Mo steel evaporator and austenitic superheater sections.

3. Both the high and low level oxygen water chemistry regimes have been shown to be successful in preventing erosion-corrosion damage (ref. 2-5), but for the combined regime adopted in the UK, which uses low oxygen levels, it is important to define the limits of its applicability, particularly since it involves dosing excess hydrazine ultimately to remove the oxygen which provides protection. Work has therefore been carried out at CERL to establish the oxygen concentrations required to inhibit erosion-corrosion under a variety of experimental conditions and in particular as a function of the metal loss rate and hydrodynamic conditions. In addition, it has sought to establish the influence of hydrazine on the process and the ability or oxygen to inhibit erosion-corrosion in the presence of excess nydrazine, particularly as a function of temperature.

4. The work has also made it possible to establish the relationship between the high and low oxygen dosing regimes, with respect to erosion-corrosion damage, and to explain why the incidence of damage can be rather variable in plant operating under nominally deoxygenated AVT water chemistry, where feedwater oxygen levels are <10 μg kg^{-1} and hydrazine is dosed as a scavenger for residual oxygen.

U.S. NUCLEAR REGULATORY COMMISSION
In the Matter of Entergy Nuclear Vermont Yankee LLC
Docket No. 50-271 Official Exhibit No. NEC-JH-72
OFFERED by: Applicant/Licensee (Intervenor) NEC
NRC Staff Other
IDENTIFIED on 7/21/08 Witness/Panel Hogenfeld
Action Taken: (ADMITTED) REJECTED WITHDRAWN
Reporter/Clerk MAC

DOCKETED
USNRC
August 12, 2008 (11:00am)
OFFICE OF SECRETARY
RULEMAKINGS AND
ADJUDICATIONS STAFF

Template Secy-028

DS-03

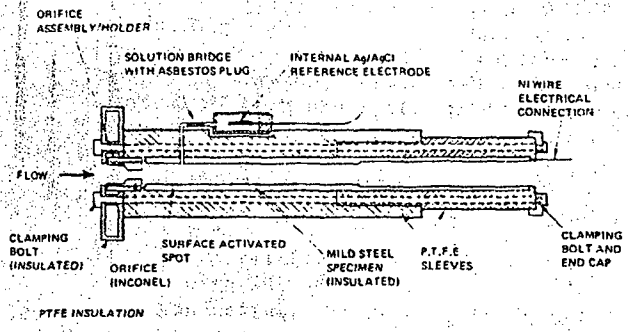

Fig. 1 Orifice assembly test specimen with electrochemical monitoring

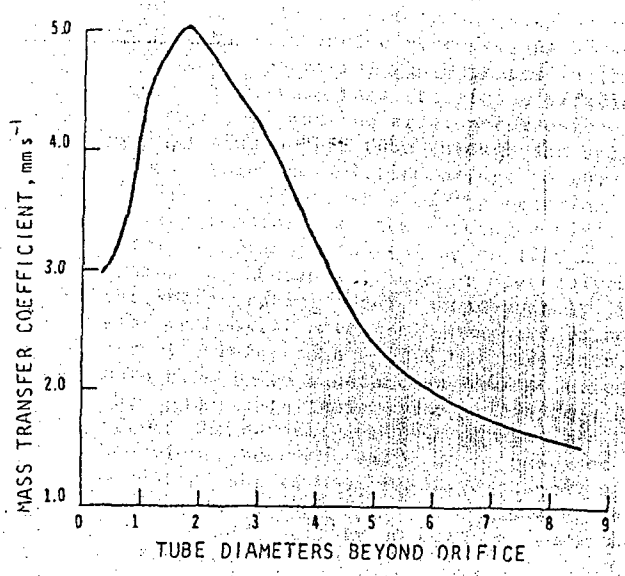

Fig. 2 Typical mass transfer coefficient variation downstream of an orifice

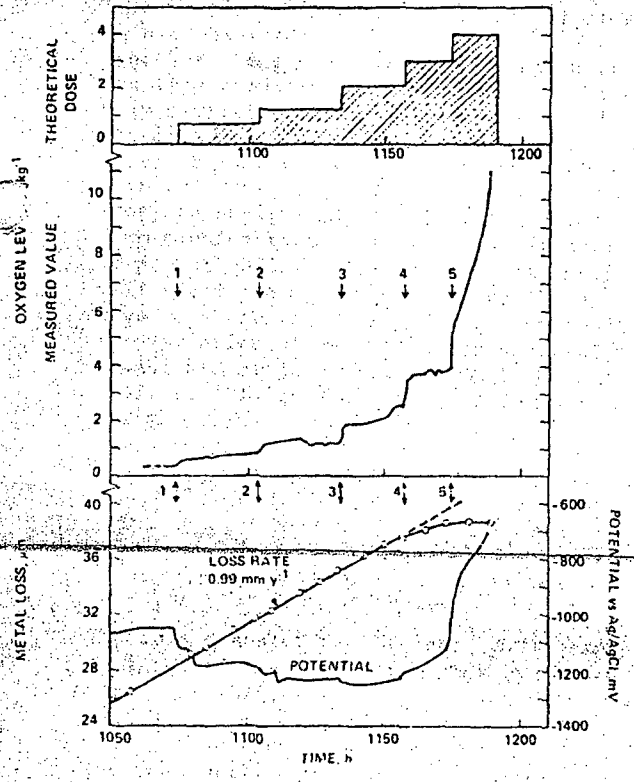

Fig. 3 Influence of oxygen on erosion-corrosion and specimen potential at 115°C
1, Start O_2 dose
2-5, O_2 dose increased

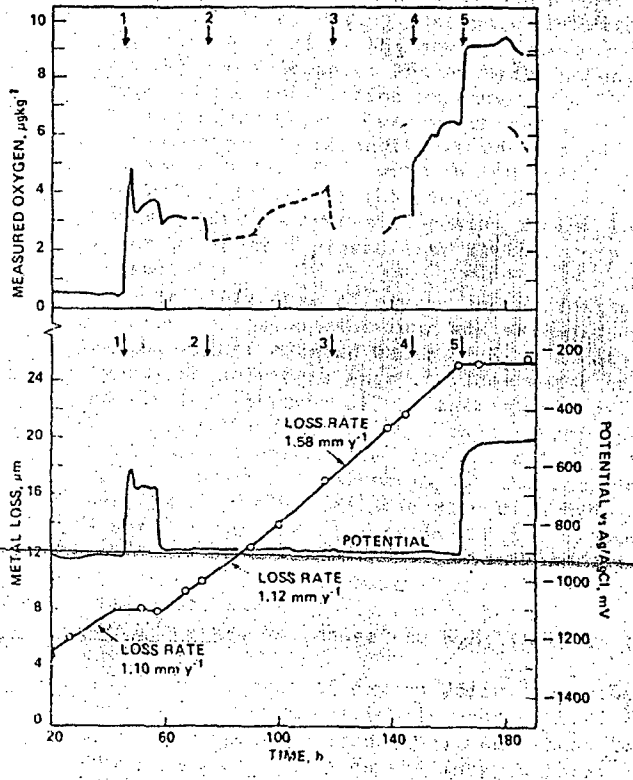

Fig. 4 Influence of oxygen on erosion-corrosion and specimen potential at 150°C
1, Start O_2 dose. 2, O_2 dose switched to 2nd flow channel. 3, O_2 dose stopped. 4, Start 2nd O_2 dose. 5, Dose increased.

EXPERIMENTAL STUDIES

5. The erosion-corrosion studies described here were carried out using the CERL high velocity isothermal water loop. Full details of the test loop have been given elsewhere (ref. 1, 8). It incorporates four main specimen flow channels, two in the main loop, and two in a secondary polishing loop. The rig is largely constructed from Type 316 stainless steel and designed to operate up to 350°C and 21.78 MN m^{-2} pressure. The experimental programme has shown it to be capable of operating for long periods with very precise control of both physical and chemical conditions. The control limits are indicated below:

- Temperature, ±1°C
- Flow to test specimens, ±1% up to 1031 kg h^{-1}
- pH of circulating water*, <±0.05 pH unit with NH_3 dosing
- Conductivity of water after cation exchange, <0.2 µS cm^{-1}
- Dissolved active silica in recirculating water, <6 µg kg^{-1}
- Dissolved Fe in circulating water*, <10 µg kg^{-1}

*Value depends on specific conditions of test, typically much lower values of dissolved Fe are obtained.

6. For the present studies, test specimens of the type shown in Fig. 1 were used. These are very similar in principle to those used previously in our experimental programme (ref. 1, 2), but have been modified to allow electrochemical monitoring of the specimen. The basic specimen design employs an inlet orifice, made from erosion resistant material (Inconel 600), to produce highly turbulent conditions in the mild steel tubing downstream, which in turn gives rise to the erosion-corrosion damage. The variation of mass transfer coefficient downstream of an orifice is well characterised (ref. 9, 10), as shown in Fig. 2, with the maximum value being defined by the relationship:

$$Sh_{max} = 0.276\ Re_N^{0.67}\ Sc^{0.33} \quad \ldots (1)$$

where Sh_{max} = maximum Sherwood number observed downstream of orifice
Re_N = orifice Reynolds number
Sc = Schmidt number

The mass transfer coefficient, K. is expressed in terms of the Sherwood number by the relationship $Sh = KD/\mathcal{D}$, where D = duct diameter and $\mathcal{D}$ = diffusion coefficient.

7. The erosion-corrosion loss in the region of the post orifice maximum was monitored in-situ by observing the activity loss from specimens which had been surface activated with ^{56}Co, as indicated in Fig. 1. Full details of the technique used have been given elsewhere (ref. 11). The loss sensitivity in the present studies was better than ±0.15 µm, allowing very accurate determination of specimen response to changes in the water chemistry and in particular to the oxygen dose level.

potentials with respect to an internal Ag/AgCl/0.01 M KCl reference electrode. As shown in Fig. 1, the potential was measured in the region of maximum mass transfer coefficient and, therefore, of maximum erosion-corrosion loss, by inserting a PTFE tube through the specimen wall to form the solution bridge to the specimen. Measurements of the chloride concentration remaining in the reference electrode after experiments lasting up to 1200 hours indicated substantial loss of electrolyte to the recirculating water. Consequently, the electrochemical potentials measured do not strictly refer to a 0.01 M KCl reference, but more closely to a saturated AgCl solution at the appropriate temperature. This does not affect the general analysis of specimen behaviour, however, since it is based on large potential shifts over relatively short periods of time (a few hours), when the electrode would have reached equilibrium with the environmental conditions.

CONDITIONS AND MONITORING OF WATER CHEMISTRY

9. The experiments described here were carried out in deoxygenated AVT feedwater, to which controlled levels of oxygen and hydrazine were then added. The pH of the recirculating water was controlled with NH_3. This was effected both by dosing make-up water with the appropriate level of NH_3 and by controlled removal and release of NH_3 by hydrogen and ammonium ion form cation exchange resin beds in the secondary water clean-up circuit. Experiments were conducted at various pHs in the range 8.0 to 9.3, with the pH typically controlled to better than ±0.05 pH units. However, during hydrazine dosing to the loop water pH control proved less satisfactory (see below).

10. The influence of oxygen and hydrazine on erosion-corrosion behaviour was examined by dosing either aerated water or N_2 sparged hydrazine solutions into the loop water approximately 1 m upstream of the test specimens. In the case of hydrazine, the reagent rapidly recirculated around the loop and a stable concentration was maintained at the test specimens by balancing the dose rate with hydrazine decomposition and removal on the ion exchange columns. Unfortunately this displaced NH_3 from the ammoniated resin making pH control more difficult, particularly during periods when it was necessary to change the N_2H_4 level in the water.

11. In the case of oxygen dosing into the loop, when it had previously been operating under deoxygenated (reducing) conditions for some time, magnetite on the loop surfaces had a substantial capacity for removing oxygen in the recirculating water. As a result of this O_2 'gettering', it was usually necessary to run at a constant O_2 dose level for some time before steady oxygen levels were established at the inlet to the test specimens. This also ensured equilibration and negligible O_2 loss in the sample lines, which were located approximately 15 cm upstream of the specimens. Valves in the

mixing of the dose and recirculating water. After prolonged periods of O_2 dosing to the loop water, it was found to recirculate around the loop and the O_2 level at the test specimens rose cumulatively, as indicated in Fig. 3.

12. Because of the difficulties of sampling and measuring O_2 at the very low levels involved in the present work, great care was taken to ensure the accuracy of such measurements by multiple method determination at various points in the loop circuit. Samples were drawn continuously from a sampling point at the inlet to the test specimen in the flow channel being dosed and from an equivalent point in the parallel flow channel ahead of a second test specimen. This provided a check on oxygen recirculation around the loop and allowed 'differential' experiments to be conducted where erosion-corrosion was maintained in the undosed flow channel, but inhibited in the dosed one. The O_2 concentration in the recirculating water was also monitored downstream of the ion exchange column in the polishing loop by batch analysis and on a continuous basis in some experiments.

13. The oxygen levels quoted in the present paper were measured using an Orbisphere model 2713 membrane polarographic O_2 monitor. Measurements were normally made with a total sample flow rate of around 80 ml min^{-1} and a flow of 9 ml min^{-1} through the monitor itself. With flow rates of this order and strenuous efforts to ensure minimum O_2 ingress on the low pressure side of the sampling system, measured O_2 levels in He sparged 'blank' water were typically in the range 0.2 to 0.3 µg kg^{-1}. Similar values were obtained from loop water after operation under deoxygenated conditions for a few days. With lower sample flow rates slightly higher oxygen levels were observed. Oxygen measurements obtained using the continuous autoanalyser version of the leuco-methylene blue method (ref. 12) were in good agreement with those obtained using the Orbisphere instrument and indicated the absolute values to be accurate to about ±0.5 µg kg^{-1} in the 0 to 10 µg kg^{-1} range.

14. As noted earlier, the absolute O_2 levels measured may be unrepresentative of that reaching the specimen if significant oxygen consumption occurs within the sample lines. As a rule, therefore, several hours equilibration were allowed at any given oxygen dose level to ensure that the O_2 level determined was indeed representative of that reaching the specimen. Typically, however, when O_2 dose levels were changed, the majority of the increment was seen within an hour or so. In those cases where O_2 recirculation around the loop could be demonstrated not to have occurred, the oxygen levels were cross checked by comparison with the theoretical values expected from the O_2 dose rate. Fig. 3 shows a good example of such a comparison for O_2 dosing at 115°C. Only at the end of the dosing period is O_2 recirculation evident and prior to this agreement between measured and theoretical O_2 levels is good.

15. At temperatures of 180°C and above, increased O_2 consumption by loop surfaces and sample lines made reliable oxygen measurements more difficult. Under these circumstances, it was necessary to use the theoretical oxygen level derived from the dose rate to give an upper limit for the oxygen level at the test specimen. While this allowed demonstration of effects due to low levels of O_2, equivalent to those observed at lower temperature, it precluded accurate quantitative assessment. Similarly, it was not possible to measure oxygen concentrations in the presence of hydrazine at these temperatures and data again had to be related to the theoretical O_2 dose. At 150°C and below, however, the hydrazine-oxygen reaction was sufficiently slow to allow measurement of O_2 in the presence of hydrazine. In both cases it was possible to demonstrate clearly the effects of oxygen in the presence of excess hydrazine.

16. Hydrazine in loop water was monitored continuously using the p-dimethylamino-benzaldehyde hydrazone auto-analyser method (Technicon Auto Analyser Industrial Method No. 147-71WM, 1973). Hydrogen in the loop water was determined by gas chromatography of the dissolved gases, which had been stripped from the sample water by diffusion through a silicone rubber membrane into a helium carrier gas (ref. 13). It was not possible to control hydrogen in the loop water and its concentration increased progressively with temperature as a result of the increased corrosion of steel surfaces in the loop (from around 15 µg kg^{-1} at 115°C to 90 µg kg^{-1} at 210°C).

RESULTS AND DISCUSSION

Influence of Oxygen on Erosion-Corrosion

17. Fig. 3 shows the influence of a progressively increasing O_2 dose on a specimen undergoing rapid erosion-corrosion loss (0.99 mm $year^{-1}$) at 115°C and pH 9.1. The O_2 level was progressively increased to 2.1 µg kg^{-1} without any noticeable effect on the erosion-corrosion rate over a period of about 70 hours. However, the specimen showed a progressive shift to more negative potentials with increasing oxygen level over this range. This effect has been noted previously at low temperature (ref. 2), but its origin is unclear at present. Increasing the O_2 concentration to 3.8 µg kg^{-1} can be seen to have caused a reduction in the erosion-corrosion rate over a period of 24 hours and shifted the specimen potential more positive again. In view of the continuing positive drift of the specimen potential at the end of this period, it is possible that further exposure at this oxygen concentration would have stopped the erosion-corrosion loss eventually. However, increasing the concentration to no more than 6.2 µg kg^{-1} caused the potential to shift sharply more positive and stopped further erosion-corrosion loss. Oxygen recirculation around the loop prevented more precise control of the O_2 concentration and hence more accurate definition of the concentration required to inhibit attack.

18. Fig. 4 shows similar data for O_2 inhibition of erosion-corrosion at 150°C and at a rather lower pH, around 7.8. The low pH adopted in this case was to ensure high erosion-corrosion rates at this temperature. The initial oxygen

dose starting after 45 hours (4.9 μg kg^{-1}) immediately caused the ongoing erosion-corrosion loss of 1.10 mm $year^{-1}$ to be inhibited. Reduction of the oxygen concentration to around 3.5 μg kg^{-1} continued to inhibit the process and to maintain the much more positive specimen potential. However, reducing the oxygen concentration to 3.2 μg kg^{-1} allowed erosion-corrosion to reinitiate rapidly, at a rate similar to that seen previously. At the time, the specimen potential was seen to shift sharply negative to a value similar to that observed prior to O_2 dosing. Subsequently, the erosion-corrosion rate increased to 1.58 mm $year^{-1}$ and continued at this value during oxygen dosing until the O_2 concentration was raised above 6.5 μg kg^{-1}. Again, the positive shift in specimen potential and cessation of erosion-corrosion loss was almost immediate on raising the concentration above the threshold.

19. Experiments of the type described above have been repeated many times at these two temperatures with essentially the same result, except that the O_2 threshold for inhibition of erosion-corrosion varied with the loss rate and mass transfer coefficient to the specimen surface. At higher temperatures, up to 250°C, the results were similar, but obtaining an oxygen threshold was more difficult due to the difficulties in oxygen determination and the low erosion-corrosion rates encountered.

20. It is important to note that the oxygen dosing experiments at 115°C and 150°C were carried out with 10 to 20 μg kg^{-1} dissolved hydrogen in the loop water. This represents a large excess of H_2 over the O_2 concentrations used to inhibit erosion-corrosion, typically an order of magnitude greater than that required to combine with the oxygen via the formal reaction:

$$H_2 + \tfrac{1}{2}O_2 \rightarrow H_2O \qquad \ldots (2)$$

Nevertheless, it was still the oxygen present which controlled the specimen electrochemical potential and erosion-corrosion behaviour. This was also found to apply at temperatures up to 250°C and with even larger excesses of hydrogen (up to 2 orders of magnitude). It should also be noted that these H_2 levels are of course higher than those normally encountered in boiler feedsystems.

21. The rapid shift in electrochemical potential to much more positive potentials and the inhibition of the erosion-corrosion process above a threshold O_2 concentration is consistent with a switch in the cathodic reaction of the corrosion process from hydrogen evolution to oxygen reduction. That is,

$$\text{From } 2H^+ + 2e \rightarrow H_2 \qquad \ldots (3)$$
$$\text{To } \tfrac{1}{2}O_2 + H_2O + 2e \rightarrow 2OH^- \qquad \ldots (4)$$

In the case of active erosion-corrosion, the cathodic hydrogen evolution reaction (3) is balanced by an equal and opposite anodic one leading to the dissolution of iron as Fe^{2+} species. The latter is generally agreed to occur via the reductive dissolution of the magnetite corrosion film formed on the metal surface (ref. 2).

22. The specimen electrochemical behaviour is also consistent with the rate of oxygen reduction being controlled by the rate of oxygen mass transfer to the specimen surface. A reasonable initial approach to assessing the oxygen concentration necessary to inhibit any given erosion-corrosion rate is, therefore, to compare the rate under fully deoxygenated conditions with the rate of oxygen mass transfer to the specimen surface required to inhibit the process. This is, to equate the anodic reaction rate with the equivalent cathodic reaction (4), which would have been required to balance it if the erosion-corrosion loss had continued unaffected. i.e.

$$K_{O_2}[\bar{O}_2]\rho_w \equiv \text{Erosion-Corrosion Rate} \qquad \ldots (5)$$

where K_{O_2} = local oxygen mass transfer coefficient

$[\bar{O}_2]$ = concentration of oxygen in solution required to inhibit the erosion-corrosion loss

ρ_w = density of water.

If the relationship given in equation (5) holds, then plots of the oxygen threshold versus (Erosion-Corrosion Rate)/$\rho_w K_{O_2}$ should give a straight line of slope 0.285, defined by the equivalent weights of Fe and O_2 in the corrosion process.

23. Fig. 5 and 6 show plots for the influence of oxygen on erosion-corrosion rate derived from our data at 115°C and 150°C, respectively. The mass transfer coefficients for oxygen were calculated using the expression given in equation (1), taking the diffusion coefficients for oxygen (K_{O_2}) as 8.8×10^{-9} m^2 s^{-1} and 1.27×10^{-8} $m^2 s^{-1}$ at 115° and 150°C, respectively (ref. 15). Other aqueous constants were taken from standard steam tables. Since the threshold itself is not as readily defined as the alternatives where erosion-corrosion continues unaffected or is completely inhibited, Figs. 5 and 6 are constructed on the latter basis, the threshold being the boundary line between the two zones. As expected there is a band of uncertainty associated with this, defined by the half closed symbols and the dashed lines.

24. At both 115° and 150°C there is clearly an oxygen concentration threshold below which erosion-corrosion is unaffected and above which the process is inhibited, which can be defined in terms of the pre-existing erosion-corrosion rate and the rate of oxygen mass transfer to the surface. However, the slope of the threshold line is lower than that predicted by equation (5), by a factor of 4 for the correlation at 150°C, which represents the better data set. It is important to point out, however, that the experimentally determined erosion-corrosion rate is equated to a theoretically derived rate of oxygen mass transfer. For many corrosion processes, such close agreement between experiment and theory would be considered sufficient to confirm the theoretical analysis. However, examination of the possible errors involved in the estimation of oxygen mass transfer and erosion-corrosion rate, indicates that the deviation of the slope of the threshold lines from the predicted value of 0.285 is real. Thus rather less oxygen is

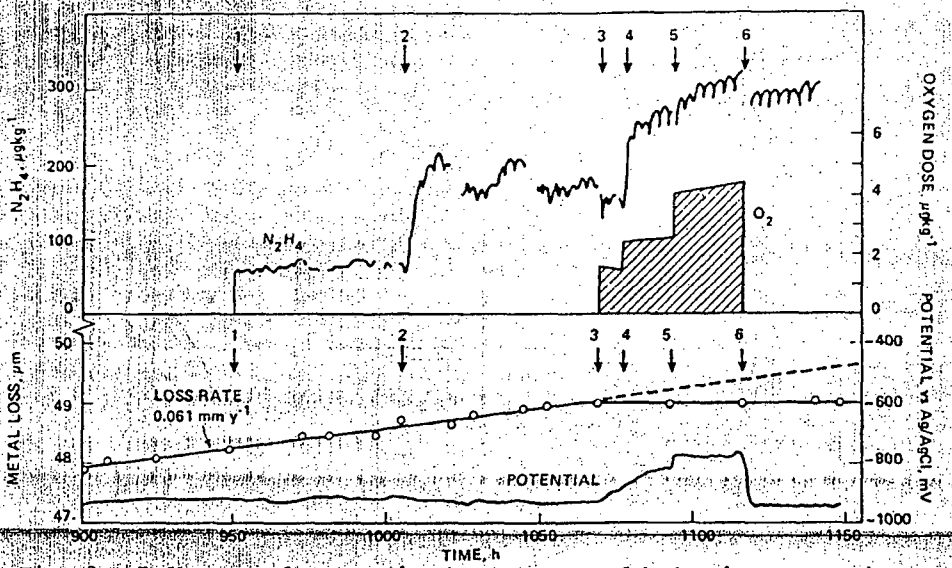

Fig. 8 Influence of oxygen in the presence of hydrazine on erosion-corrosion and specimen potential at 210°C.
1, Start N_2H_4 dose. 2, N_2H_4 dose increased. 3, Start O_2/N_2H_4 dose. 4 & 5, O_2/N_2H_4 dose increased. 6, O_2 dose stopped.

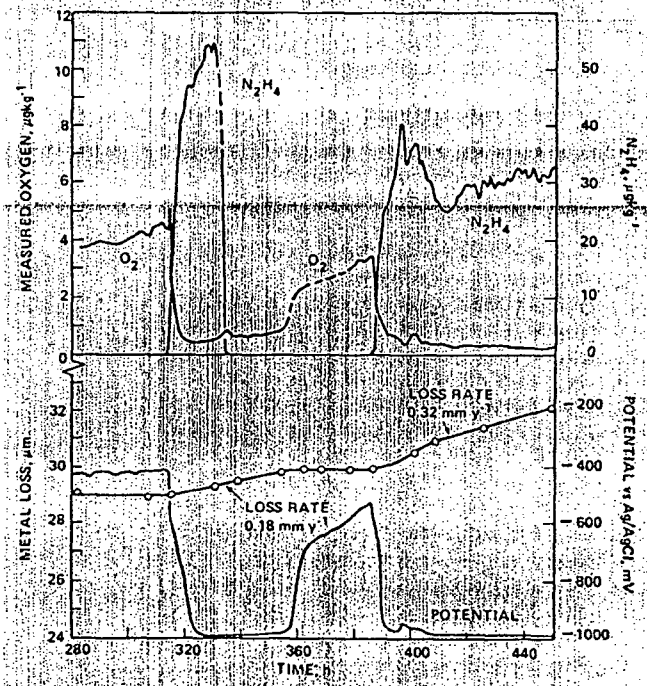

Fig. 9 Effect of hydrazine on erosion-corrosion and specimen potential due to removal of oxygen at 150°C

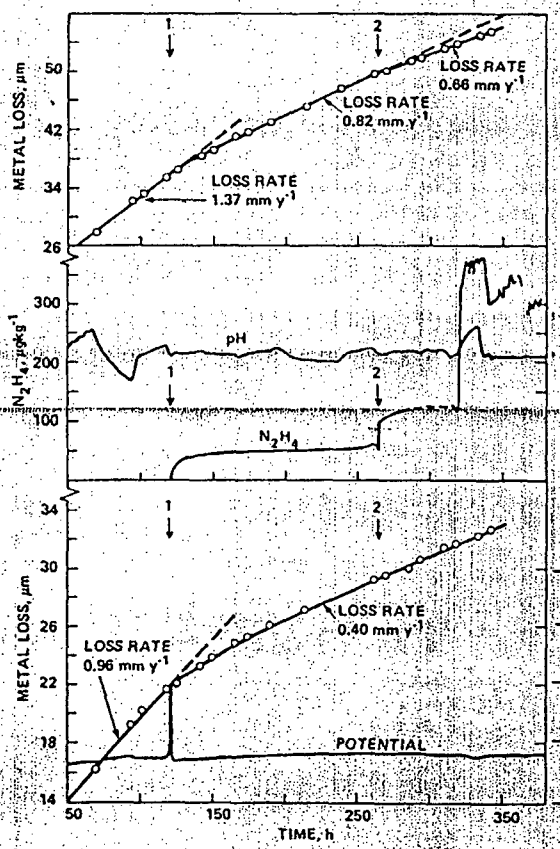

Fig. 10 Effect of hydrazine on erosion-corrosion and specimen potential in absence of oxygen at 180°C
1, Start N_2H_4 dose. 2, Dose increased.

required to inhibit erosion-corrosion than would be predicted by equating the loss rate to the rate of oxygen mass transfer to the surface. The latter does appear to represent an upper limit to the amount required for inhibition though.

25. Whether the O_2 threshold for inhibition eases with increasing temperature as indicated by Figs. 5 and 6 is uncertain. The data at 115° and 150°C can be treated as a single set, but there is then greater scatter of the threshold values. It may at first seem surprising that the O_2 thresholds are less than those predicted by the mass transfer analysis, but it appears to be consistent with the mechanism proposed for the erosion-corrosion process by the present authors (ref. 1, 2). In effect the process is self accelerating, due to the need to evolve hydrogen at progressively more negative potentials in order to match the anodic dissolution rate. This, in turn, raises the solubility of the magnetite corrosion film, allowing even higher mass transfer limited dissolution rates. When oxygen reduction starts to compete with hydrogen evolution as the cathodic reaction, the potential will start to shift in the positive direction, reducing the solubility of the magnetite film. This, in turn, will lead to further reductions in the mass transfer limited dissolution process and, as the oxygen level is increased further, to a very sharply reducing erosion-corrosion loss rate. Our observation of a relatively narrow range of oxygen concentrations over which the loss rates are reduced, but which do not completely inhibit the process, appears to match this view of the inhibition mechanism. Further analysis of this aspect of erosion-corrosion behaviour is under investigation.

26. As drawn, Figs. 5 and 6 show a positive intercept of 1.5 μg kg^{-1} for the O_2 threshold at zero erosion-corrosion rate. Equation (5) predicts that the intercept should be zero. Part of this offset may be accounted for by the positive 'blank' oxygens measured, typically 0.2 to 0.3 μg kg^{-1}, and by the difficulties of accurate measurements at such very low oxygen concentrations. However, the data do not preclude the possibility that the threshold rises more rapidly at these very low O_2 concentrations, with a rather lower intercept than that indicated. This would be consistent with the view that for very low erosion-corrosion rates, where the self accelerating mechanism of the process is much less important, the threshold approximates more closely to that given by equation (5).

Influence of Oxygen in the Presence of Hydrazine

27. As noted earlier, oxygen is effective in inhibiting erosion-corrosion in the presence of excess hydrogen. Fig. 7 shows the influence of oxygen in the presence of a vast excess of hydrazine at 180°C. It was not possible to measure the oxygen level reaching the specimen, due to the reaction with hydrazine in the rig between dosing and sampling point) and down the sample line. Consequently, the Fig. 7. This represents the upper limit of O_2 which could have been present at the specimen, but even these modest levels (<7 μg kg^{-1}) were sufficient to inhibit an ongoing erosion-corrosion rate of 0.79 mm $year^{-1}$ in the presence of around 180 μg kg^{-1} N_2H_4. Fig. 8 shows that oxygen is equally effective at 210°C for inhibiting erosion-corrosion in the presence of around 300 μg kg^{-1} N_2H_4, although the loss rates were much lower at this temperature. In both cases there was also a large excess of hydrogen present over the oxygen concentration (H_2 ~ 90 μg kg^{-1} at 210°C). It is clear, therefore, that low levels of oxygen control the incidence of erosion-corrosion even in the presence of huge excesses of the two common reducing agents likely to be present in boiler feedwater, namely H_2 and N_2H_4, and our data shows this to be the case up to 250°C.

28. Since oxygen is the potential controlling species with carbon steel up to 250°C, it is likely that other corrosion or oxide deposition processes are influenced by very low levels of oxygen in the feedwater, even though excess H_2 or N_2H_4 may be present. Of course, these reducing agents will remove O_2 from the feedwater given sufficient time, but the reaction kinetics are sufficiently slow, particularly at the lower temperature end of our investigations, that O_2 can penetrate many metres through the feed system and into the boiler. It is, therefore, clear why haematite is frequently observed in the low temperature (<250°C) parts of power plant boiler and feed systems, even with nominally deoxygenated feedwater and added hydrazine. The data of Ribon and Berge (ref. 15) provide a good example of such behaviour in a conventional boiler operating with a deoxygenated AVT feedwater chemistry with addition of hydrazine. Up to 265°C, haematite was the major oxide phase observed in corrosion product samples taken from the boiler system. Above this temperature magnetite predominated. It is also clear why zones of active erosion-corrosion damage, where the metal surface is covered with magnetite, can be surrounded by adjacent ones covered by haematite. While oxygen levels are insufficient to inhibit damage in the highly turbulent regions, they are sufficient to shift the surface potential to more positive values in areas of lower mass transfer and, hence, to lead to the formation of haematite. Similarly, some boiler feed systems operating with nominally 'deoxygenated' feedwater may suffer serious erosion-ocorrosion problems, whilst others which are apparently similar, but in reality have slightly higher feedwater oxygens, show none.

29. When reaction times are long enough, Fig. 9 shows that hydrazine will efficiently remove O_2 at low levels (<5 μg kg^{-1}) and allow erosion-corrosion to reinitiate rapidly.

Direct Influence of Hydrazine on Erosion-Corrosion

30. Fig. 10 shows the influence of hydrazine on erosion-ocorrosion in the absence of oxygen (<0.5 μg kg^{-1}) at 180°C and essentially

15. RIBON C. and BERGE J.Ph. Magnetite deposits in boilers from iron in solution. Proc. Am. Power Conf., 32, 721, 1970

16. COBBLE J.W. and TURNER P.J. Additives for pH control in PWR secondary water. EPRI Report NP-4209